Characterization of the Phosphate Units in Rat Dentin by Solid-State NMR Spectroscopy

Yao-Hung Tseng,[†] Yi-Ling Tsai,[†] Tim W. T. Tsai,[†] John C. H. Chao,[†] Chun-Pin Lin,*[‡]
Shih-Hao Huang,[‡] Chung-Yuan Mou,[†,§] and Jerry C. C. Chan*[†]

*Department of Chemistry, School of Dentistry, and Center of Condensed Matter, National Taiwan
University, No. 1, Section 4, Roosevelt Road, Taipei 10617, Taiwan*

Dentin samples of the incisor taken from Wistar rats of different ages are studied. A series of physical techniques are used to characterize the samples, with particular emphasis on ^{31}P solid-state nuclear magnetic resonance. The structure of incisor dentin in rats can be described as apatite crystallites embedded in an amorphous matrix. We find that 19% of the apatite crystallites contain hydroxyl groups, which are distributed near the surface of the crystallites. The internal region of the crystallites is deficient in hydroxyl groups. As rats mature with age, there are several changes in the chemical composition of the incisor dentin: (i) the water content and phosporous amount in the amorphous matrix decrease; (ii) the amount of the phosphorus species in the apatite crystallites remains the same; and (iii) the loss of phosphorus species is accompanied by approximately the same loss of the calcium content.

Introduction

Studies of calcified tissues are of important interest to the development of biomaterials. There are three distinct biological minerals in an individual tooth, namely, enamel, dentin, and cementum. The chemical composition of dentin is quite similar to that of bone, containing 70 wt % of inorganic phase, 20 wt % of organic matrix, and 10 wt % of water.[1] The inorganic phase of tooth dentin was identified as calcium phosphate with an apatite structure.[2] After decades of efforts, however, the composition and structure of this biological mineral remain poorly characterized at the molecular level. The major difficulty is that a significant structural disorder is commonly found in biological hard tissues, and therefore the utility of diffraction techniques is very limited.

The usefulness of solid-state nuclear magnetic resonance (NMR) spectroscopy has been well recognized in the field of biomineralization. After the pioneering ^{31}P solid-state NMR works on hydroxyapatite (HAp) and its nonstoichiometric forms,[3] there is a large body of literature on the ^{31}P NMR studies of calcified tissues.[4–14] There are many different NMR methods developed to probe for the PO_4^{3-} and HPO_4^{2-} units in apatitic materials, including cross-polarization (CP) with dipolar dephasing,[4] differential CP,[7] adiabatic demagnetization in the rotating frame,[15] deconvolution of the variable-contact-time CP curve,[13] and heteronuclear correlation (HETCOR) spectroscopy.[8,16] The excellent review by Kolodziejski has provided a comprehensive account of solid-state NMR studies of calcified tissues.[12] Most of these NMR works, however, focus on bone and enamel only. Because the chemical compositions of dentin and bone are quite similar, it is of great interest to apply ^{31}P solid-state NMR spectroscopy to characterize the phosphate species in dentin and to compare the results with those reported for bone. Furthermore, it is very difficult to quantify different ^{31}P species in biominerals because of their structural disorder. Although one may compare the ^{1}H and ^{31}P magic-angle spinning (MAS) spectra to quantify different ^{31}P species in nanocrystalline HAp,[16] this method may not be applicable to biominerals because of the inherent poor spectral resolution in the ^{1}H dimension. Recently, Cho et al. have shown that HETCOR is very useful for characterizing the phosphate species in the apatite domain of bone

* Corresponding authors. E-mail: chanjcc@ntu.edu.tw (J.C.C.C.); pinlin@ha.mc.ntu.edu.tw (C.-P.L.).
† Department of Chemistry.
‡ School of Dentistry.
§ Center of Condensed Matter.

(1) LeGeros, R. Z. *Calcium Phosphates in Oral Biology and Medicine*; Karger: Basel, 1991.
(2) Mann, S. *Biomineralization - Principles and Concepts in Bioinorganic Materials Chemistry*; Oxford University Press: New York, 2001.
(3) Rothwell, W. P.; Waugh, J. S.; Yesinowski, J. P. *J. Am. Chem. Soc.* **1980**, *102*, 2637.
(4) Aue, W. P.; Roufosse, A. H.; Glimcher, M. J.; Griffin, R. G. *Biochemistry* **1984**, *23*, 6110.
(5) Roufosse, A. H.; Aue, W. P.; Roberts, J. E.; Glimcher, M. J.; Griffin, R. G. *Biochemistry* **1984**, *23*, 6115.
(6) Santos, R. A.; Wind, R. A.; Bronnimann, C. E. *J. Magn. Reson., Ser. B* **1994**, *105*, 183.
(7) Wu, Y.; Glimcher, M. J.; Rey, C.; Ackerman, J. L. *J. Mol. Biol.* **1994**, *244*, 423.
(8) Cho, G. Y.; Wu, Y. T.; Ackerman, J. L. *Science* **2003**, *300*, 1123.
(9) Wu, Y.; Ackerman, J. L.; Strawich, E. S.; Rey, C.; Kim, H. M.; Glimcher, M. J. *Calcif. Tissue Int.* **2003**, *72*, 610.
(10) Kaflak-Hachulska, A.; Samoson, A.; Kolodziejski, W. *Calcif. Tissue Int.* **2003**, *73*, 476.
(11) Jäger, C.; Groom, N. S.; Bowe, E. A.; Horner, A.; Davies, M. E.; Murray, R. C.; Duer, M. J. *Chem. Mater.* **2005**, *17*, 3059.
(12) Kolodziejski, W. Solid-state NMR studies of bone. In *Top. Curr. Chem.*; Klinowski, J., Ed.; Springer Verlag: Berlin, 2005; Vol. 246, pp 235–270.
(13) Kaflak, A.; Chmielewski, D.; Gorecki, A.; Slosarczyk, A.; Kolodziejski, W. *Solid State Nucl. Magn. Reson.* **2006**, *29*, 345.
(14) Wilson, E. E.; Awonusi, A.; Morris, M. D.; Kohn, D. H.; Tecklenburg, M. M. J.; Beck, L. W. *Biophys. J.* **2006**, *90*, 3722.
(15) Ramanathan, C.; Ackerman, J. L. *J. Magn. Reson.* **1997**, *127*, 26.
(16) Jäger, C.; Welzel, T.; Meyer-Zaika, W.; Epple, M. *Magn. Reson. Chem.* **2006**, *44*, 573.

SSNMR Study of Rat Dentin

Chem. Mater., Vol. 19, No. 25, 2007 6089

material,[8] which represents the first quantitative analysis of phosphorus species in biominerals. However, its basic assumption that only apatite and its OH-deficient variant are present may not be justified for some biominerals.

In this work, we have developed a more general NMR strategy for the quantitative analysis of phosphorus species in biominerals. Dentin samples of the incisor taken from Wistar rats of different ages were chosen for our study. Rat incisor is "rootless" in which the root canal is open and the tooth continues to grow indefinitely. Our experimental data show that the water content and the amount of phosphorus species are significantly different in these samples, revealing a change in the metabolic activities in rat incisors of different ages.

Experimental Section

Sample Preparation and Characterization. Hydroxyapatite ($Ca_{10}(PO_4)_6(OH)_2$), monetite ($CaHPO_4$), and brushite ($CaHPO_4 \cdot 2H_2O$) were used as received (Acros Organics). A sample of octacalcium phosphate (OCP) was prepared as described previously.[17] Dentin samples were taken from the incisors of Wistar rats, which were 7 mm long and 1.2 mm wide (Supporting Information). After the enamel layer was removed by a high-speed dental bur, the samples were washed with saline three times and then ground into powder form by a grinder (Mortar Grinder KM 100). X-ray diffraction (XRD) measurements were performed on a Philips X'Pert diffractometer, using Cu Kα radiation ($\lambda = 1.5418$ Å). The field emission scanning electron microscopy (FE-SEM) and the energy dispersive X-ray (EDX) analysis were done on a JEOL-JSM-6700F field emission scanning electron microscope (operating at 10 kV) equipped with an Oxford INCA energy dispersive X-ray spectrometer. For each sample, the EDX measurements were repeated at different locations five times. The dentin samples ashed at 800 °C were dissolved in 2% HNO_3 solution for inductively coupled plasma mass spectrometry (ICP-MS) measurements, which were performed on a Perkin-Elmer Elan 6000 system. The standard solutions of 1000 mg/L Ca^{2+} and Mg^{2+} (Merck) were diluted into ppb levels for the calibration measurements. Thermogravimetric (TG) analyses were carried out on a DuPont951 thermogravimetric analyzer with a heating rate of 10 K/min.

Solid-State NMR. All NMR experiments were measured at room temperature and carried out at ^{31}P and ^1H frequencies of 121.5 and 300.1 MHz, respectively, on a Bruker DSX300 NMR spectrometer equipped with commercial 4-mm and 2.5-mm probes. The sample was confined to the middle one-third of the rotor volume using Teflon spacers. The variation of MAS frequency was limited to ±3 Hz using a commercial pneumatic control unit. Chemical shifts were externally referenced to 85% phosphoric acid and tetramethylsilane for ^{31}P and ^1H, respectively. The $^{31}P\{^1H\}$ double-quantum (DQ) filtered Lee–Goldburg (LG) CP HECTOR spectra were measured at a spin rate of 10 kHz using the 4-mm probe. During the contact time the ^1H nutation frequency and the resonance offset were set equal to 50 and 35.35 kHz, respectively, to fulfill the LG irradiation condition.[18] The ^{31}P DQ filter was prepared on the basis of the finite-pulse radio frequency-driven recoupling (fpRFDR) technique.[19,20] During the fpRFDR recoupling periods,
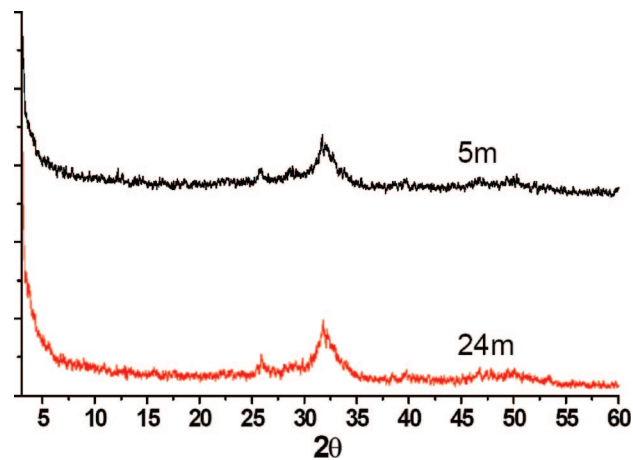

Figure 1. XRD patterns of the 5-m and 24-m samples.

the ^{31}P π pulses were set to 30 μs ($\tau_p/\tau_r = 0.3$).[21] The π pulse trains were phase cycled according to the XY-8 scheme.[22] The ^{31}P $\pi/2$ pulses flanking the fpRFDR pulse blocks were set to 5 μs.[19] The DQ reconversion period was set equal to the excitation period. Proton decoupling was set to 85 kHz during the DQ excitation/reconversion periods. Typically, for each t_1 increment 32 transients were accumulated, and a total of 50 increments were done at steps of 100 μs. A more detailed description of the DQ-filtered LG-CP HETCOR experiment was given elsewhere.[23]

The ^{31}P spin–echo–dipolar–dephasing experiments were measured using the 2.5-mm probe at a spin rate of 25 kHz. The ^{31}P $\pi/2$ and π pulses were set to 5 and 10 μs long, respectively. The ^1H nutation frequency was set to 25 kHz during the interpulse delay and then to 80 kHz afterward. The recycle delay was set to 600 s. The ^{31}P spin–lattice relaxation times were determined by the saturation-recovery technique.[24] All the intensity data had been normalized by the sample mass and corrected for the organic content in dentin.

Results and Analysis

XRD, EDX, ICP-MS, and TG. Dentin samples of 3 weeks, 5 months, and 24 months old Wistar rats are labeled as the 3-w, 5-m, and 24-m samples, respectively. The eruption rate of the incisors of Wistar rats is about 2.8 mm per week. The 3-w, 5-m, and 24-m samples correspond to the dentins of young, mature, and old rats. The XRD patterns of our sample series are shown in Figure 1. There are two broad peaks positioned at 2θ equal to 26 and 32°. The poor resolution of the diffraction patterns could be attributed to the nanosize and/or strain of the crystallites. Our results are quite similar to what have been observed for the mineral phase of human dentin.[1] No appreciable difference is observed for the XRD patterns of the 5-m and 24-m samples. A typical SEM image measured for the 24-m sample is shown in Figure 2, where the region for EDX analysis has been highlighted. The Ca/P and Ca/Mg ratios determined

(17) Tseng, Y. H.; Zhan, J. H.; Lin, K. S. K.; Mou, C. Y.; Chan, J. C. C. *Solid State Nucl. Magn. Reson.* **2004**, *26*, 99.
(18) Lee, M.; Goldburg, W. I. *Phys. Rev. A* **1965**, *140*, 1261.
(19) Ishii, Y.; Balbach, J. J.; Tycko, R. *Chem. Phys.* **2001**, *266*, 231.
(20) Oyler, N. A.; Tycko, R. *J. Phys. Chem. B* **2002**, *106*, 8382.

(21) Ishii, Y. *J. Chem. Phys.* **2001**, *114*, 8473.
(22) Gullion, T.; Baker, D. B.; Conradi, M. S. *J. Magn. Reson.* **1990**, *89*, 479.
(23) Tseng, Y.-H.; Tsai, Y.-L.; Tsai, T. W. T.; Lin, C.-P.; Huang, S.-H.; Mou, C.-Y.; Chan, J. C. C. *Solid State Nucl. Magn. Reson.* **2007**, *31*, 55.
(24) Freeman, R. *Spin Choreography: Basic Steps in High Resolution NMR*; Oxford University Press: New York, 1998.
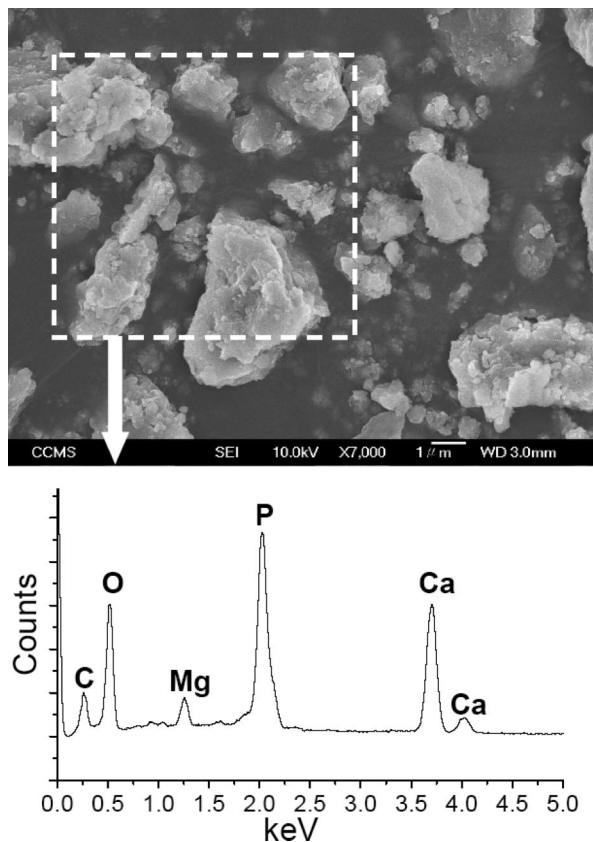
Figure 2. SEM image and the EDX data of the 24-m sample.

Table 1. Ca/P and Ca/Mg Ratios Determined for the Dentin Samples

	EDX		ICP-MS
sample	Ca/P	Ca/Mg	Ca/Mg
3-w	1.37 ± 0.03	17 ± 3	10.2 ± 0.3
5-m	1.39 ± 0.02	9.3 ± 0.7	8.9 ± 0.2
24-m	1.42 ± 0.02	8.3 ± 0.7	8.5 ± 0.2

for our dentin samples are summarized in Table 1. The Ca/ Mg ratios were also determined by ICP-MS. The Ca/Mg ratios determined by EDX and ICP-MS for the 3-w sample are different, presumably reflecting the heterogeneous distribution of Mg^{2+} ions in dentin. The Ca/P ratios are approximately the same for our dentin samples, whereas the Ca/Mg ratios of the 5-m and 24-m samples are significantly lower than that of the 3-w sample. The organic contents of all the dentin samples were found to be 22.5 wt %.

$^{31}P\{^{1}H\}$ LG CP HETCOR. The ^{31}P and ^{1}H MAS spectra of the dentin samples were measured at a spin rate of 10 kHz, with very limited resolution. For the ^{1}H MAS spectra (Supporting Information), the signal at 6.5 ppm with significant spinning sidebands can be assigned to structural water with restricted motion,[25,26] although the minor contribution from the organic matrix of dentin cannot be excluded. The analysis of ^{31}P MAS spectra is severely plagued by the poor resolution usually encountered in biomineral samples, but $^{31}P\{^{1}H\}$ HETCOR can effectively alleviate the resolution problem.[6,8] To suppress the spin
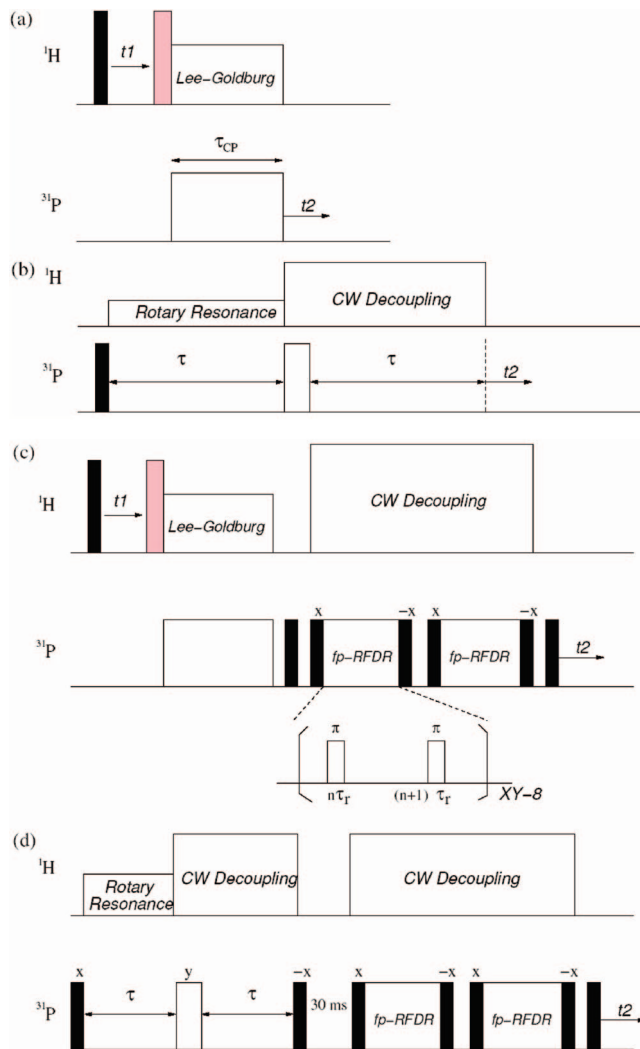
(25) Yesinowski, J. P.; Eckert, H. *J. Am. Chem. Soc.* **1987**, *109*, 6274.
(26) Lin, K. S. K.; Tseng, Y. H.; Mou, Y.; Hsu, Y. C.; Yang, C. M.; Chan, J. C. C. *Chem. Mater.* **2005**, *17*, 4493.

Figure 3. Pulse sequences employed in this work. All the filled rectangles represent $\pi/2$ pulses of 5 μs. The unspecified delays between some of the pulse blocks are in the range from 2 to 10 μs. (a) LG-CP HETCOR. The rectangles in grey represent the pulse with flip angles adjusted to bring the ^{1}H magnetization spin locked along the effective field. (b) Spin–echo–dipolar–dephasing experiment. The rotary resonance condition was achieved by setting the ^{1}H nutation frequency equal to the spinning frequency. The interpulse delays (τ) were set to 4, 5, 6, 7, and 8 ms. (c) DQF LG-CP HETCOR. The duration of the π pulses within the fpRFDR blocks were set equal to 30% of the rotor period. There is a 30 ms z-filter inserted before the reading pulse. (d) DQ excitation with T_2 filtering. The τ values were set to 4 ms for our measurements.

diffusion among the ^{1}H spins during the CP contact time, the LG irradiation was applied in the ^{1}H channel as shown in Figure 3a. Figure 4 shows the $^{31}P\{^{1}H\}$ LG-CP HETCOR spectrum of the 24-m sample measured at a spin rate of 10 kHz. There are two major spectral components at ^{1}H chemical shifts of 0.2 and 6.5 ppm, namely, the apatite and amorphous components, respectively. The apatite component is a well-known spectral marker of the apatite domain.[25] In this work, the phosphorus species of the apatite domain refer to PO_4^{3-} in close proximity to OH^{-} ions or to H_2O molecules located at the hydroxyl sites of the HAp lattice. The amorphous component is assigned to the disordered phase which contains a substantial amount of structural water and phosphorus species. To quantify the intensities of these two components, which may have very different CP dynamics, we measured the HETCOR spectra at different contact times.

SSNMR Study of Rat Dentin

Chem. Mater., Vol. 19, No. 25, 2007 6091

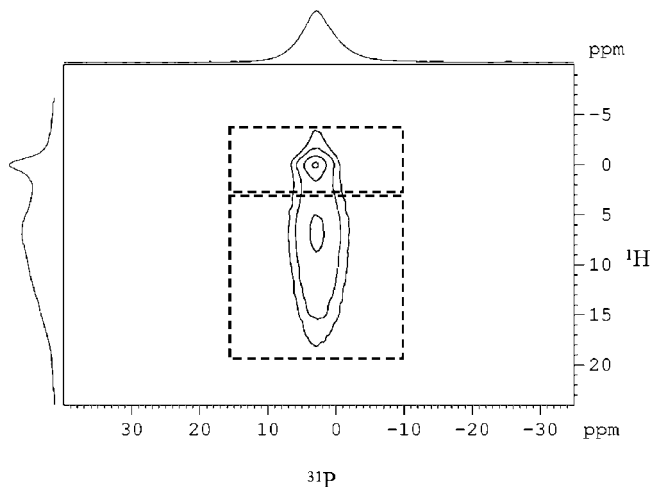**Figure 4.** $^{31}P\{^1H\}$ LG-CP HETCOR spectrum of the 24-m sample with contact time equal to 2 ms. The signal contributions from the apatite and amorphous components were obtained by integrating the two rectangular regions centered at the ^1H chemical shifts of 0.2 and 11 ppm, respectively.

The intensities of the two components at different contact times were obtained by integrating the highlighted regions in Figure 4, which were then fitted by the following equation:

$$M(t) = M_0\{1 - \exp(-t/\tau_{CP})\} \exp(-t/T_{1\rho}^H)$$

where M_0 is the intensity factor of arbitrary unit; τ_{CP} characterizes the rate constant of the polarization transfer between the ^{31}P and ^1H species; and $T_{1\rho}^H$ reveals the relaxation behavior of the ^1H species in the spin-locking rf field. The parameter M_0 can be used to quantify the relative amount of the species being analyzed. Although the amorphous component has a shoulder at 13 ppm which is most likely due to HPO_4^{2-}, the spectral resolution does not allow us to separately quantify its contribution. Additional HETCOR measurements with frequency-switched LG irradiation applied during the t_1 evolution gave a similar spectral resolution in the region of 13–16 ppm, just as what have been reported for bone samples.[14]

In the following, we will separately discuss the CP dynamics of the apatite and amorphous components in the HETCOR spectra. Similar to HAp, the $T_{1\rho}^H$ values of the apatite component were too long to be characterized by our experimental setup for all the dentin samples. Referring to Figure 5, the τ_{CP} data obtained are identical within experimental error, which are invariably smaller than the τ_{CP} value obtained for a commercial HAp sample under the same experimental condition. This observation can be accounted for by the fact that the hydroxyl groups of the apatite lattice may well be substituted by water molecules.[10] The τ_{CP} and $T_{1\rho}^H$ data obtained for the amorphous component are summarized in Figure 6, in which the data obtained for monetite and brushite are included for comparison. The $T_{1\rho}^H$ value of the 24-m sample is significantly larger than those of the 3-w and 5-m samples, revealing a considerable decrease in the water content for the 24-m sample. The τ_{CP} values decrease monotonically from the 3-w to the 24-m sample, indicating a gradual increase in the interaction between the phosphorus and the proton species. Because the τ_{CP} value of the 24-m sample is similar to those of brushite or monetite, the most
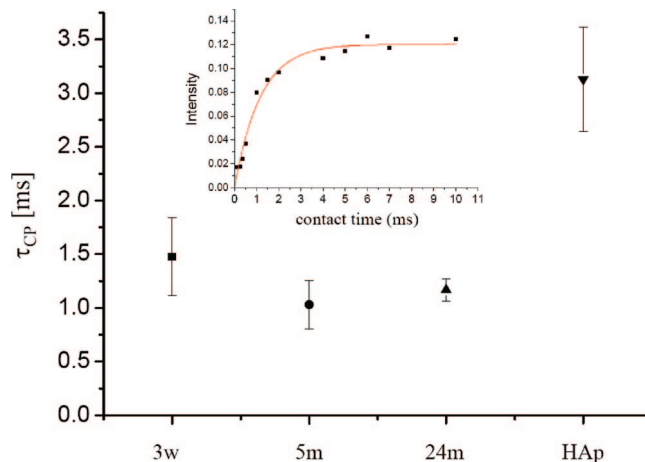

Figure 5. Data of τ_{CP} obtained for the apatite component of the variable contact-time LG-CP HETCOR spectra. The inset shows a typical fitting of the raw data.
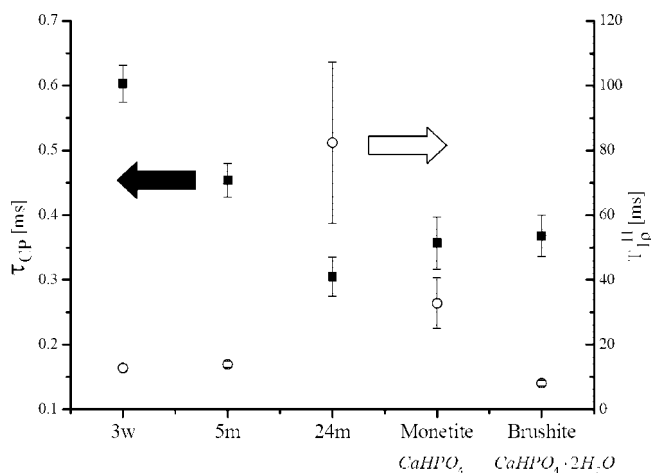

Figure 6. Data of τ_{CP} and $T_{1\rho}^H$ obtained for the amorphous component of the variable contact-time LG-CP HETCOR spectra.

plausible rationalization is that the amorphous component of the 24-m sample is mainly comprised of the HPO_4^{2-} species. The 3-w and 5-m samples, on the other hand, contain a substantial amount of $HO-H\cdots O-PO_3^{3-}$ in the amorphous phase.

Quantification of ^{31}P Species. To quantify the various ^{31}P species in dentin, we employed a commercial HAp sample as our spin-counting standard. The ^{31}P spin–lattice relaxation time of HAp was determined to be 88 s, and those obtained for our dentin samples ranged from 68 to 78 s. We first determined the total phosphorus amount by Bloch decay (one-pulse) experiments with recycle delay set to 600 s. The contribution of the ^{31}P signal from the organic component is expected to be negligible.[12] To probe for the ^{31}P species which are remote from any protons, we used the spin–echo technique incorporated with a ^1H rotary resonance sequence during the interpulse delay (spin–echo–dipolar–dephasing). The pulse sequence is shown in Figure 3(b). As a preliminary test, it was found that a spin–echo delay of 4 ms is long enough to suppress the PO_4^{3-} signal of HAp or the HPO_4^{2-} signal of OCP. Therefore, any measurements with the spin–echo delay longer than 4 ms can be used to quantify the ^{31}P species remote from protons. We repeated the
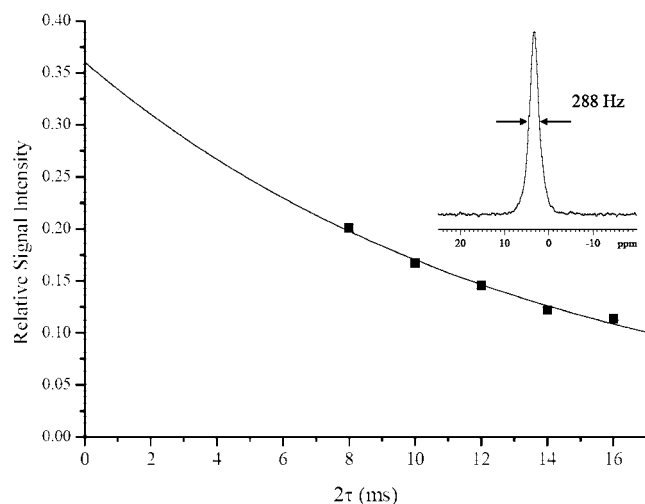
Figure 7. Signal intensities of the spin–echo–dipolar–dephasing experiment measured for the 3-w sample. The intensities as a function of twice the interpulse delay (2τ) were fitted by an exponential decay curve to mimic the effect of T_2 relaxation. The intensity extrapolated at $2\tau = 0$ represents the amount of the phosphorus species remote from protons. The inset shows the spectrum obtained at $2\tau = 8$ ms.

measurements at different spin–echo delays, namely, 4, 5, 6, 7, and 8 ms. These signal intensities were then fitted by an exponential decay curve as shown in Figure 7. The value extrapolated at vanishing spin–echo delay reveals the intensity free from transverse relaxation effect. The acquired ^{31}P spectra invariably contain a single sharp peak at 3.2 ppm, with line width at half-maximum equal to 288 Hz (2.4 ppm). The relatively narrow line width indicates that the phosphorus species are of crystalline nature. We have compiled a list of crystalline phosphate compounds related to biominerals (Supporting Information). From the NMR data of brushite and OCP,[9,17] it is established that HPO_4^{2-} species would have ^{31}P chemical shifts ≤ 2 ppm. The ^{31}P MAS spectrum of β-tricalcium phosphate contains multiple peaks in the range of 0–6 ppm.[27] The ^{31}P chemical shifts of other possible candidates such as $Mg_3(PO_4)_2$ are outside the range of 2.8–3.5 ppm.[28,29] Therefore, the sharp ^{31}P signal at 3.2 ppm is assigned to OH-deficient apatite, in which the OH^- ions may be substituted by different anions such as carbonate or fluoride.[1] Additional measurements on model compounds such as carbonate HAp are required to confirm the assignment. Table 2 summarizes the amounts of different phosphorus species. The overall phosphate content decreases from the 3-w to the 24-m sample by 12%, which is mainly due to the decrease of the phosphorus content in the amorphous phase. Note that the loss of phosphorus species is accompanied by approximately the same loss of the calcium content because of the invariance in the Ca/P ratio. From the amounts of the apatite component and its OH-deficient analogue, it is further deduced that 19% of the total apatite crystallites contain OH^- ions for all the samples.

^{31}P{^{1}H} DQ-Filtered LG-CP HETCOR. Distance distributions of phosphorus species in bone and enamel can be well characterized by the van Vleck second moments (M_2),[30] which can be obtained by measuring the ^{31}P spin–echo amplitudes as a function of echo time under static condition.[31] However, this approach will not produce very informative results for our dentin samples unless the ^{31}P signals at different proton environments can be distinguished. Therefore, the resolution enhancement demonstrated in the LG-CP HETCOR spectrum is exploited to determine the ^{31}P–^{31}P second moments of the apatite component. The idea is to add a DQ filter after the LG-CP HETCOR module. Figure 3c shows the pulse sequence we used to measure the DQ-filtered LG-CP HETCOR (DQF-HETCOR) spectra. A series of DQF-HETCOR spectra were measured at different excitation and reconversion times to create the desired DQ excitation profiles. Empirically, a DQ excitation profile can be analyzed by the following equation:[26,32,33]

$$I(\tau_{exe}) = A\tau_{exe}^2 \exp\{-\tau_{exe}^2/B\}$$

where the rate of the initial DQ signal buildup is described by the parameter A, which is proportional to the M_2 value of the interacting nuclear spins; the constant B describes the decay of the DQ signal. A more detailed description of the data analysis is given elsewhere.[23] Table 3 summarizes the parameters A and B obtained for our dentin samples. Calibration measurements on commercial HAp sample can be used to extract the ^{31}P–^{31}P second moments for the apatite component.[23] Because the amorphous component contains both $HO-H\cdots O-PO_3^{3-}$ and HPO_4^{2-} ions, it is rather difficult to find a suitable model compound to extract its M_2 value from the parameter A. Referring to Table 3, the M_2 value of the apatite component determined for the 3-w sample is $(6.8 \pm 0.4) \times 10^6$ rad^2/s^2, which is somewhat smaller than that of crystalline HAp. This observation is in accordance with the fact that some of the phosphate ions in biological apatites are substituted by carbonate ions.[1] On the other hand, it is surprising that the M_2 value obtained for the apatite component of the 24-m sample is larger than that of HAp by 43%. It is inconceivable that the density of the phosphorus species in the apatite phase can have any significant increase without affecting the apatitic structure. From the ^{31}P chemical shifts, the presence of other high M_2 species such as pyrophosphate or $Ca(H_2PO_4)_2$ can also be ruled out unequivocally.[3,29] Previously, we have shown for HAp that a spinning frequency of 25 kHz can significantly enhance the ^{31}P–^{31}P DQ excitation efficiency, causing the A value to increas from 10.6 to 21.4 ms^{-2}.[23] Such enhancement is due to the suppression of the ^{31}P chemical shift anisotropy by the fpRFDR pulse symmetry at high spinning frequency. We therefore speculate that the PO_4^{3-} units in the 24-m sample are undergoing molecular motions, leading to a reduction of the chemical shift anisotropy and hence an increase in the DQ excitation efficiency. Additional experi-

(27) Obadia, L.; Deniard, P.; Alonso, B.; Rouillon, T.; Jobic, S.; Guicheux, J.; Julien, M.; Massiot, D.; Bujoli, B.; Bouler, J. M. *Chem. Mater.* **2006**, *18*, 1425.

(28) Aramendia, M. A.; Borau, V.; Jimenez, C.; Marinas, J. M.; Romero, F. J.; Ruiz, J. R. *J. Solid State Chem.* **1998**, *135*, 96.

(29) Scrimgour, S. N.; Chudek, J. A.; Lloyd, C. H. *Dent. Mater.* **2007**, *23*, 415.

(30) Abragam, A. *Principles of Nuclear Magnetism*; Clarendon Press: Oxford, 1961.

(31) Wu, Y. T.; Ackerman, J. L.; Kim, H. M.; Rey, C.; Barroug, A.; Glimcher, M. J. *J. Bone Miner. Res.* **2002**, *17*, 472.

(32) Schmedt auf der Günne, J.; Eckert, H. *Chem.—Eur. J.* **1998**, *4*, 1762.

(33) Tseng, Y.-H.; Mou, C.-Y.; Chan, J. C. C. *J. Am. Chem. Soc.* **2006**, *128*, 6909.

SSNMR Study of Rat Dentin

Chem. Mater., Vol. 19, No. 25, 2007   6093

Table 2. Relative Amount of Phosphorus Species in Rat Dentins Determined by NMR Spin-Counting

phosphorus species	HAp	3-w	5-m	24-m
M_0 (apatite component)[a]		0.20 ± 0.02	0.18 ± 0.01	0.12 ± 0.01
M_0 (amorphous component)[a]		1.33 ± 0.06	1.04 ± 0.06	0.64 ± 0.03
all phosphorus[b,c]	1.00	0.98	0.92	0.86
phosphorus remote from protons[b,d,e]		0.36 ± 0.02	0.35 ± 0.03	0.34 ± 0.01
phosphorus close to protons[f]		0.62 ± 0.02	0.57 ± 0.03	0.52 ± 0.01
apatite component[g]		0.08 ± 0.01	0.08 ± 0.01	0.08 ± 0.01
amorphous component[g]		0.54 ± 0.04	0.49 ± 0.04	0.44 ± 0.03

[a] The M_0 values were determined from the variable contact-time LG-CP HETCOR experiments. [b] All the data had been normalized by the sample mass and corrected for the organic content in dentin (ca. 22.5 wt %). All data were referenced to a commercial HAp sample. [c] Determined by ^{31}P Bloch decay experiments with recycle delay set equal to 600 s. [d] Determined by spin–echo dipolar dephasing experiments. [e] Identifiable to OH-deficient apatite. [f] A simple subtraction of the fourth-row entries from the third-row entries. [g] Determined from the fifth-row entries on the basis of the M_0 ratio of the apatite and amorphous components.

Table 3. Fitting Parameters for the Buildup of the DQ Excitation Profile and the Extracted ^{31}P-^{31}P van Vleck Second Moments

	apatite component			amorphous component	
sample	A (ms^{-2})	B (ms^2)	$M_2 \times 10^6$ (rad^2/s^2)	A (ms^{-2})	B (ms^2)
HAp	10.6 ± 0.5	6.6 ± 0.2	7.70^a		
3-w	9.3 ± 0.2	4.7 ± 0.1	6.8 ± 0.5^b	7.6 ± 0.3	5.3 ± 0.1
5-m	12.0 ± 0.8	4.8 ± 0.2	$8.7 \pm 0.7^{b,c}$	8.6 ± 0.7	5.3 ± 0.3
24-m	15.2 ± 0.5	4.8 ± 0.3	$11.0 \pm 0.6^{b,c}$	11.4 ± 0.8	5.3 ± 0.3

[a] The M_2 value was calculated on the basis of the crystal structure (ref 38). [b] The proportionality constant between A and M_2 is obtained by comparing the A value and the calculated M_2 value of HAp. [c] The apparent M_2 value may not correspond to the true M_2 value (see the text).

Table 4. Calculated ^{31}P-^{31}P Second Moments of Several Optimized Structures of Carbonated HAp[a]

carbonate substitution in HAp	charge compensation	^{31}P-^{31}P $M_2 \times 10^6$ (rad^2/s^2)[b]
A: $OH^- \Rightarrow CO_3^{2-}$	$-OH^-$	6.10
B1: $PO_4^{3-} \Rightarrow CO_3^{2-}$	$-OH^- - Ca^{2+}$	5.01
B2: $2PO_4^{3-} \Rightarrow 2CO_3^{2-}$	$-Ca^{2+}$	3.95
B3: $PO_4^{3-} \Rightarrow CO_3^{2-}$	$-Ca^{2+} + H^+$	5.26

[a] The coordinates of the optimized structures were taken from the literature.[35] [b] The M_2 values were calculated on the basis of all the ^{31}P-^{31}P distances within 20 Å. An average of the M_2 values was taken for the cases of multiple phosphorus sites.

ments at different temperatures are required to corroborate this tentative interpretation.

OH-Deficient Apatite. On the basis of the chemical shift information, we assigned the single sharp peaks of the spin–echo–dipolar–dephasing spectra to OH-deficient apatite. To probe for any variation in the ^{31}P-^{31}P M_2 values in this phase, we add a DQ filter after the spin–echo–dipolar–dephasing module ($\tau = 4$ ms) as shown in Figure 3d. Using the procedure described above, the ^{31}P-^{31}P M_2 values of (3.6 ± 0.3), (3.9 ± 0.3), and $(3.2 \pm 0.3) \times 10^6$ rad^2/s^2 were obtained for the 3-w, 5-m, and 24-m samples, respectively. The M_2 values are substantially smaller than that of HAp, showing that significant amount of the phosphate sites in the OH-deficient apatite are substituted by other species such as carbonate ions. Contrary to what we found for the apatite component, the M_2 values of the OH-deficient apatite component are very similar for the 3-w, 5-m, and 24-m samples. This is an indication that the OH-deficient apatite is in the core of the apatite crystallites and therefore the corresponding M_2 values are not affected by the variation of the chemical composition in the amorphous matrix.

Discussion

Phosphorus Species in Dentin. Cho et al. measured a series of HETCOR spectra and analyzed the intensities of the signals arising from the apatite phase. They concluded that only 21% of the apatite crystallites in bone contain hydroxyl groups.[8] Although the amount of $HO-H\cdots O-PO_3^{3-}$ and HPO_4^{2-} are indeed very minor in the bone samples studied by Cho et al., it is not generally the case for biominerals. Our data show that the phosphorus species in the amorphous phase account for more than 50% of the total phosphorus amount in rat dentin. After explicitly taking $HO-H\cdots O-PO_3^{3-}$ and HPO_4^{2-} into account, we find

that 19% of the apatite crystallites in our dentin samples contain hydroxyl groups, quite similar to the result reported for bone minerals.[8] Furthermore, we find that the total amount of $HO-H\cdots O-PO_3^{3-}$ and HPO_4^{2-} decreases as rat dentins mature with age, consistent with the earlier Fourier transform infrared results of bone.[34] Because of their disorder nature, it is very difficult to separately quantify the amounts of $HO-H\cdots O-PO_3^{3-}$ and HPO_4^{2-} in the amorphous phase. Nevertheless, our τ_{CP} data allow us to conclude that in the 24-m sample the amount of $HO-H\cdots O-PO_3^{3-}$ is significantly less than that of HPO_4^{2-}.

Rat Dentin Structure. Our data show that there are four different phosphate species in rat dentin, namely, $HO-H\cdots O-PO_3^{3-}$, HPO_4^{2-}, apatitic PO_4^{3-}, and OH-deficient apatitic PO_4^{3-}. Because of the relatively large amount of the amorphous phase, the structure of incisor dentin in rats can be described as nanosized apatite crystallites embedded in an amorphous matrix containing a significant amount of $HO-H\cdots O-PO_3^{3-}$ and HPO_4^{2-} species. The OH-deficient apatite phase is distributed in the internal region of the apatite crystallites. Our second moment data show that the extent of carbonate substitution is more significant in the internal region than the outer region of the apatite crystallites. Astala and Stott have employed first principles calculations to investigate different possible arrangements of the CO_3^{2-} ions in both A- and B-type carbonated HAp.[35] The calculated ^{31}P-^{31}P M_2 values of the energetically most stable structures are summarized in Table 4. On the basis of the experimental ^{31}P-^{31}P M_2 values, it appears that the OH-deficient apatite phase in rat dentin is best modeled by the B-type carbonated HAp, for which the charge compensation is realized by removing the OH^- and Ca^{2+} species. However, the descriptors "internal" and "outer"

(34) Rey, C.; Shimizu, M.; Collins, B.; Glimcher, M. J. *Calcif. Tissue Int.* **1991**, *49*, 383.

(35) Astala, R.; Stott, M. J. *Chem. Mater.* **2005**, *17*, 4125.

regions of the apatite crystallites may be an oversimplification. Other filtering techniques[36] in NMR may reveal more structural domains in the apatite crystallites.

Biological Roles of the Amorphous Phase and Water. Very recently, water has been listed as one of the fundamental building blocks of bone.[14] If we adopt the viewpoint that water molecules play a significant role in the mineralization process of biological apatites,[37] it is reasonable to surmise further that the amorphous matrix of dentin is responsible for the teeth growth. In particular, water molecules in the amorphous matrix may allow the diffusion and storage of calcium and phosphate ions in the process of mineralization. We suggest that the structural water molecules play a prominent role at the early stage of dentin development and the mechanical properties of teeth are deteriorated with age because of the loss of structural water. Our EDX data show that the Ca/P ratios are approximately the same for our dentin samples. That is, the loss of the phosphate content approximately reflects the same percentage loss of the Ca content. If we assume that the Mg content does not change appreciably in all the dentin samples, the observed data trend of the Ca/Mg ratio also reflects the loss of Ca. It is remarkable to find that there is a continuous loss of structural water, phosphorus, and calcium content in the dentin of a rat incisor over its life span, revealing a change in its metabolic events. Most of these changes occur in the amorphous phase, and the phosporous and water contents of the apatite crystallites remain more or less unchanged.

Conclusion

Solid-state NMR spectroscopy has become a standard analytical technique for the study of biominerals because the method is noninvasive and no chemical pretreatment is required for the analysis. This feature is particularly important for systems in which water molecules are an important constituent to be analyzed. In this work, we have developed a solid-state NMR strategy for the quantification of phosphorus species in different environments. Our approach is readily applicable to the study of bone minerals. Overall, the structure of incisor dentin in rats can be described as nanosized apatite crystallites embedded in an amorphous matrix containing a significant amount of $HO–H\cdots O–PO_3^{3-}$ and HPO_4^{2-} species. About 19% of the apatite crystallites contain hydroxyl groups, and these apatite crystallites are distributed near the surface of the crystallites. In the internal region of the crystallites, OH^- groups are low in abundance. We suggest that the $HO–H\cdots O–PO_3^{3-}$ species in the amorphous phase of dentin are crucial for the continuous growth of rat incisor.

Supporting Information Available: Pictures of the rat incisors, ^{31}P and ^1H MAS spectra, and a list of the crystalline compounds related to biominerals (PDF). This material is available free charge via the Internet at http://pubs.acs.org.

CM070531N

(36) Huang, S.-J.; Tseng, Y.-H.; Mou, Y.; Liu, S.-B.; Huang, S.-H.; Lin, C.-P.; Chan, J. C. C. *Solid State Nucl. Magn. Reson.* **2006**, *29*, 272.
(37) Neuman, W. F.; Neuman, M. W. *The Chemical Dynamics of Bone Mineral*; University of Chicago Press: Chicago, 1958.
(38) Sudarsanan, K.; Young, R. A. *Acta Crystallogr. B* **1969**, *25*, 1534.